



Contents lists available at ScienceDirect

Chinese Chemical Letters

journal homepage: www.elsevier.com/locate/ccl

A fluorogenic probe for SNAP-tag protein based on ESPT ratiometric signals

Jin Li^{a,b,c}, Qinglong Qiao^b, Yiyan Ruan^{b,c}, Ning Xu^b, Wei Zhou^b, Guixin Zhang^{d,*},
Jingli Yuan^a, Zhaochao Xu^{b,*}

^a State Key Laboratory of Fine Chemicals, School of Chemistry, Dalian University of Technology, Dalian 116024, China

^b CAS Key Laboratory of Separation Science for Analytical Chemistry, Dalian Institute of Chemical Physics, Chinese Academy of Sciences, Dalian 116023, China

^c University of Chinese Academy of Sciences, Beijing 100049, China

^d General Surgery Department, The First Affiliated Hospital of Dalian Medical University, Dalian 116011, China



ARTICLE INFO

Article history:

Received 6 January 2023

Revised 22 February 2023

Accepted 24 February 2023

Available online 2 March 2023

Keywords:

Fluorogenic probe

Ratiometric

ESPT

SNAP-tag

Wash-free imaging

ABSTRACT

Protein self-labeling tags achieve selective fusion and labeling of target proteins through genetic coding technology, but require exogenous fluorescent probes with fluorogenicity for protein tag binding to have the performance of wash-free fluorescence imaging in live cells. In this paper, we reported a fluorogenic probe **1** capable of ratiometric fluorescence recognition of SNAP-tag proteins. In this probe, the *O*⁶-benzylguanine derivative of 3-hydroxy-1,8-naphthalimide underwent a selective covalent linkage reaction with SNAP-tag protein. The hydroxyl group on the naphthalimide fluorophore formed a hydrogen bond with the functional group near the protein cavity. The excited state proton transfer occurred after illumination, to obtain the ratio fluorescence signal from blue emission to red emission, realizing the wash-free fluorescence imaging of the target proteins.

© 2023 Published by Elsevier B.V. on behalf of Chinese Chemical Society and Institute of Materia Medica, Chinese Academy of Medical Sciences.

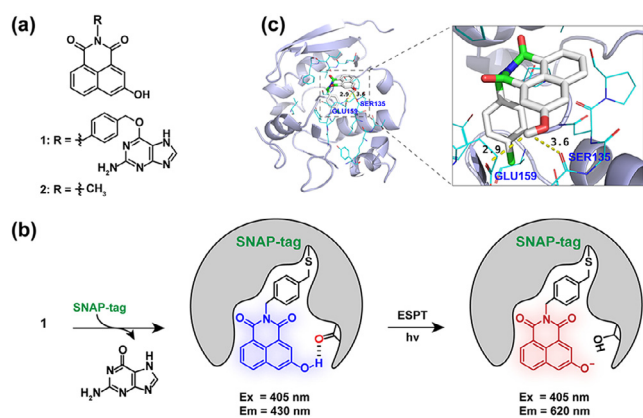
Fluorescence imaging has become the main technical method for molecular positioning and resolution of molecular interactions in cell research, which benefits from the advancement of fluorescent probes and microscopy techniques [1–8]. Fluorescent probes for functional proteins have received special attention [9,10], and various techniques such as protein self-labeling tags, bioorthogonal reactions, click chemistry and unnatural amino acids have emerged to label specific functional groups or identify specific spatial positions of target proteins [11]. Protein fluorescent probes can establish a cellular network of target proteins, especially with the help of super-resolution fluorescence microscopy to break through the diffraction limit to achieve the resolution of a single protein [12,13], and can also be used to detect the microenvironment around the target protein. For example, small molecule-sensitive fluorescent response groups were introduced at specific positions of proteins through protein self-labeling tags or unnatural amino acid technology, to realize the dynamic recognition of subcellular organelles of small molecules like zinc ions or hydrogen sulfide [14,15]. The protein recognition by fluorescent probe usually requires two steps: the specific molecular recognition reaction between the functional group on the probe and the target protein

and the specific fluorescent signal change caused by the protein recognition reaction. Since the distribution and content of probes as exogenous species cannot be controlled in cells, the development of fluorogenic probes that respond to bioorthogonal recognition reactions is the key and challenge to realizing wash-free fluorescence imaging in living cells [16].

SNAP-tag is one of the most widely used protein self-labeling technologies at present. It has excellent properties such as fast bioorthogonal reaction speed, the universality of various biological systems, and easy derivatization of fluorescent probes [17]. SNAP-tag is an engineered version of the mammalian enzyme encoded by the human *O*⁶-methylguanine-DNA alkyltransferase (hAGT). The fluorescent substrate of SNAP-tag is a molecule in which a fluorophore is covalently linked to a guanine leaving group via a benzyl group. In the labeling reaction, the substituted benzyl group of the substrate is covalently attached to the SNAP-tag via a highly stable thioether bond. To eliminate the background fluorescence produced by unreacted or excess fluorescent substrates, a variety of fluorogenic probes for SNAP-tag were designed [16,18,19]. The fluorescence response mechanism of these fluorogenic probes is mainly that the polarity of the microenvironment where the fluorophore is located becomes smaller or the degree of freedom in space is limited after being connected to SNAP-tag so that the fluorophore with intramolecular charge transfer (ICT) or twisted-

* Corresponding authors.

E-mail addresses: zgx0109@yeah.net (G. Zhang), zcxu@dicp.ac.cn (Z. Xu).



Scheme 1. (a) Structures of naphthalimide-derived probe **1** and compound **2**. (b) The reaction of probe **1** with SNAP-tag. After covalently binding to the SNAP-tag protein, probe **1** displayed the ESPT process due to the localization into the polar, hydrophobic, and proton acceptor environment of the SNAP-tag. (c) Structure-function analysis of SNAP-tag fluorophore-substrate interactions. The BG-bound variant of SNAP^{C145A} (PDB entry 3KZZ) is selected as the crystal of SNAP protein for docking. SNAP protein is represented as a cartoon, and the ligands and residues are represented as sticks and lines, respectively. Putative hydrogen bonds and corresponding distances are indicated by dashed lines.

intramolecular-charge-transfer (TICT) will appear as a significant increase in fluorescence after linking with SNAP protein [20]. However, fluorescent substrates often have non-specific distribution in cells and produce changes in fluorescence enhancement to cause interference. Since the ratiometric fluorescent probe has established an internal standard that can eliminate the interference of various environmental factors including probe concentration and non-specific enrichment, the ratiometric fluorescent signal has excellent selectivity, thereby further optimizing the background interference [21,22]. In addition, ratiometric signals can also provide quantitative information on physical parameters of the microenvironment, such as polarity. However, the ratiometric fluorogenic probe for SNAP-tag has hardly been reported.

In this paper, we reported that 3-hydroxy-naphthalimide-derived SNAP-tag probe **1** underwent an excited-state intermolecular proton transfer (ESPT) process after covalent binding to SNAP proteins, accompanied by a fluorescence transition from blue to red (Schemes 1a and b). 3-Hydroxy-1,8-naphthalimide can only undergo the ESPT process in a polar environment and the presence of hydrogen bond acceptors, and the generated oxygen anions greatly increase the intramolecular charge transfer capacity, resulting in a large red shift of the fluorescence wavelength. When probe **1** was covalently linked to the SNAP protein, the benzyl group entered the protein cavity, allowing the naphthalimide fluorophore to approach the protein so that the hydroxyl group formed an intermolecular hydrogen bond with the nearby carbonyl groups of SNAP proteins, resulting in a ratiometric fluorescent signal. The molecular docking experiments confirmed the existence of carbonyl groups (GLU159 and SER135), which are near the hydroxyl group of probe **1** (Scheme 1c).

To examine the excited-state proton transfer properties of 3-hydroxy-naphthalimide, we selected compound **2** as a reference molecule and tested its spectral properties in different solvents and alkaline environments (Fig. 1 and Figs. S3–S8 in Supporting information). Among the 13 solvents tested containing water, including from weak polarity to strong polarity, aprotic solvents to protic solvents, the absorption spectra of compound **2** remained unchanged. The maximum absorption peak was 380 nm, and the corresponding fluorescence emission wavelength was around 420 nm (Figs. 1a and b). It was worth noting that only two fluorescence emission peaks, 430 nm and 620 nm, appeared in the two solvents of dimethyl sul-

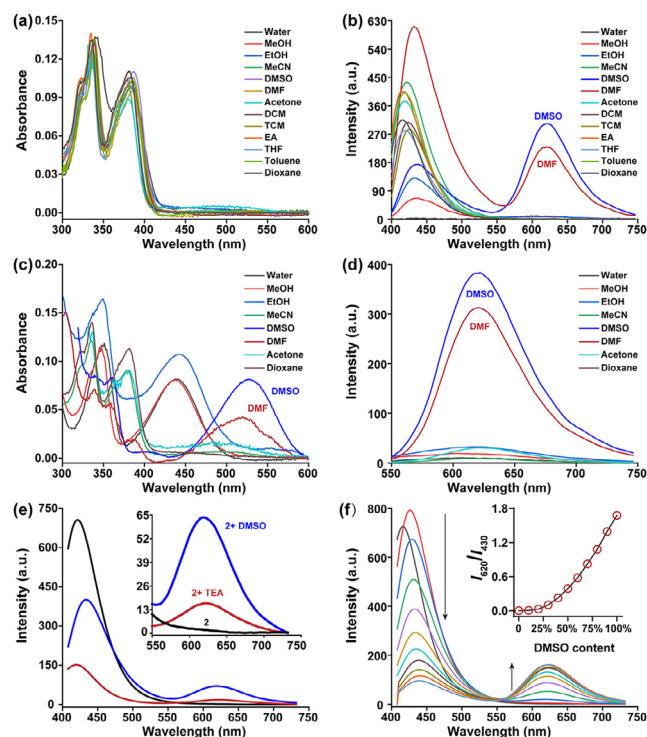


Fig. 1. Absorption and fluorescence emission spectra of compound **2**. (a) Absorption and (b) fluorescence emission spectra ($\lambda_{\text{ex}} = 380$ nm) in various solvents. (c) Absorption and (d) fluorescence emission spectra ($\lambda_{\text{ex}} = 450$ nm) after reaction with 0.1% aqueous sodium hydroxide solution (10 mmol/L). These solvents were chosen because they were soluble in water. (e) Fluorescence emission spectra before and after adding triethylamine (0.5%) and DMSO (30%) to the acetonitrile solution. (f) Fluorescence emission spectra of dioxane-DMSO system. Inset: the fluorescence intensity ratio (I_{620}/I_{430}) of the dioxane-DMSO system.

foxide (DMSO) and *N,N*-dimethylformamide (DMF). When sodium hydroxide was added to the water-miscible solvents, the maximum absorption peak of compound **2** was significantly red-shifted, and the wavelength was red-shifted to 530 nm in both DMSO and DMF (Fig. 1c). This red shift of the maximum absorption wavelength belonged to the oxygen anion species produced by removing the proton of the hydroxyl group. It was particularly important that the fluorescence peak emitted by oxyanion species in an alkaline solution was just at 620 nm (Fig. 1d), which was consistent with the long-wavelength fluorescence of compound **2** in DMSO and DMF (Fig. 1b). This indicated that the 620 nm emission of compound **2** in DMSO and DMF was due to the excited state proton transfer. The carbonyl groups of DMSO and DMF act as hydrogen bond acceptors to form intermolecular hydrogen bonds with the hydroxyl group in compound **2**. During the process of compound **2** being excited by light, the intermolecular proton transfer from compound **2** to DMSO/DMF occurred, thereby generating the oxyanion species of compound **2**. As the electrons fall back from the excited state to the ground state, the protons were retransferred from DMSO/DMF back to compound **2**. In other solvents, however, the intermolecular hydrogen bonds were weak, and no excited-state proton transfer occurred.

To further investigate the influence of intermolecular hydrogen bonds on this excited-state proton transfer process, we added DMSO to acetonitrile or dioxane, which cannot undergo excited-state proton transfer (Figs. 1e and f). The addition of triethylamine or DMSO to acetonitrile produced red fluorescence peaks at the same wavelength, which confirmed that DMSO played the role of an organic base. In dioxane, with the increase of DMSO content, the 620 nm long-wavelength fluorescence peak gradually increased,

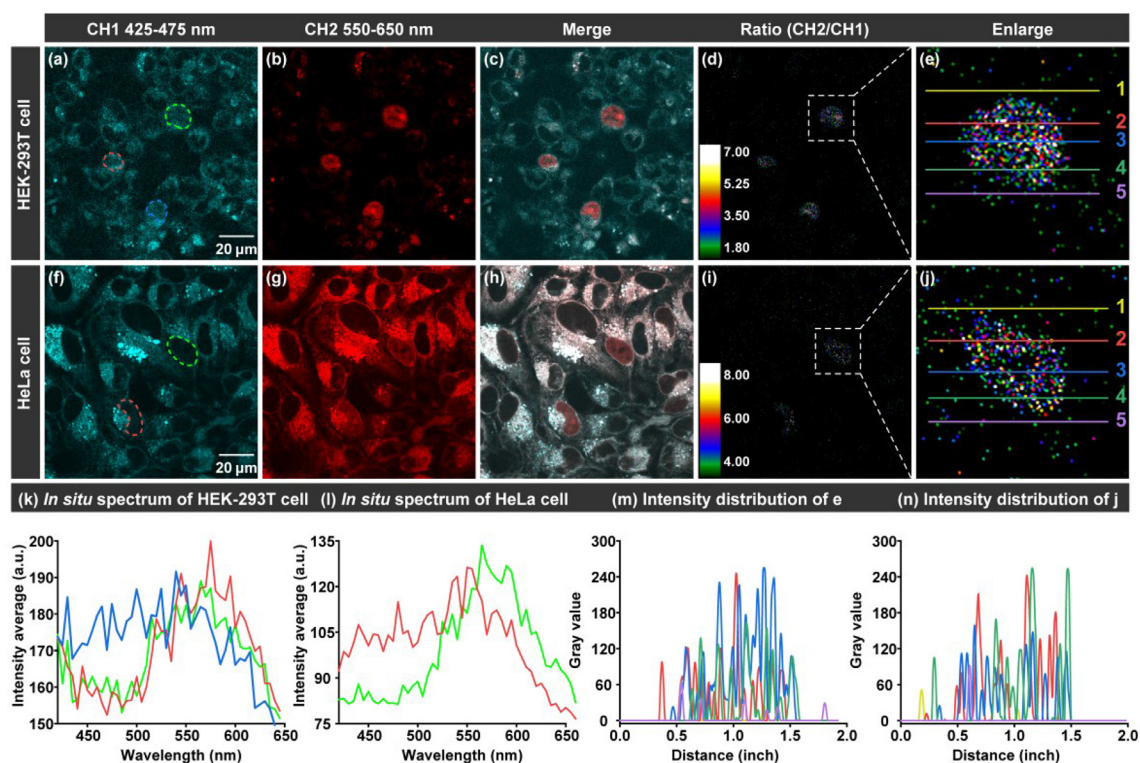


Fig. 2. Fluorescent imaging and data analysis of SNAP-tag stained with probe **1** in HEK-293T and HeLa cells. (a, f) 425–475 nm imaging channel (CH1) of HEK-293T (a) and HeLa (f) cells; (b, g) 550–650 nm imaging channel (CH2) of HEK-293T (b) and HeLa (g) cells; (c, h) the merge of images a and b (c) and images f and g (h), respectively; (d, i) ratiometric imaging of b/a (d) and g/f (i); (e, j) the enlarged image in (d) and (i), respectively; (k, l) the *in-situ* spectra of HEK-293T (k) and HeLa (l) cells; (m, n) the fluorescence intensity distribution of (e) and (j). The probe concentration was 1 $\mu\text{mol/L}$, the incubation time was 1 h, and the excitation wavelength was 405 nm. Scale bar: 20 μm .

while the 430 nm short-wavelength fluorescence peak gradually weakened, and there was an isoemission point at 550 nm. When the DMSO content exceeded 40%, the intensity ratio of the long-wavelength and short-wavelength fluorescence peaks showed a good linear relationship with the DMSO content. Compound **2** did not show long-wavelength fluorescence in sulfolane, phenyl sulfone (DPS), and diphenyl sulfoxide (DPSO), three solvents that also contained sulfur-oxygen double bonds (Fig. S9 in Supporting information), which should be due to the steric hindrance in these solvents. As a result, the hydrogen bond of these three solvents with compound **2** was not stable enough. These results fully demonstrate that the stable intermolecular hydrogen bonds determine the proton transfer process in the excited state. In addition, the photostability of the fluorophore was also investigated. As shown in Fig. S10 (Supporting information), compound **2** can maintain good photostability for 300 min after continuous xenon lamp irradiation. Although both emission peaks decreased, the ratio values remained unchanged, which highlighted the superiority of the ratio fluorophore in the field of fluorescence labeling.

There are many carbonyl groups in the protein, so we speculate that if 3-hydroxy-naphthalimide is close to the protein to form an intermolecular hydrogen bond with the carbonyl group in the protein, it can also undergo excited-state proton transfer for protein recognition. Therefore, we introduced guanine on the side of naphthalimide with benzyl as the linking group, and O^6 -benzylguanine would selectively react with SNAP protein for covalent linkage, and formed a stable thioether bond with the departure of the guanine group. We transfected the SNAP protein tag in the nuclear protein human recombinant histone H2B (H2B) of HEK-293T and HeLa cells and then stained it with probe **1** (Fig. 2). From the two wavelength fluorescence channels, we can see that the probe **1** in the cell has a wide distribution (Figs. 2a–c and f–h). However,

when collecting the ratiometric fluorescent signals between long and short wavelengths, only the nuclei transfected with SNAP protein can be imaged, while other positions of the cell and cells not transfected with SNAP protein positions had no fluorescence background interference (Figs. 2d and i). This fully demonstrates that the ratiometric fluorescence signal can effectively improve the selectivity of molecular recognition, and can realize wash-free fluorescence imaging for SNAP-tag labeled target proteins. The *in-situ* fluorescence spectra in the nucleus were collected, and it was found that the center of the long-wavelength fluorescence emission peak was around 570 nm (Figs. 2k and l), which was shorter than 620 nm in DMSO. This should be because naphthalimide is in the cavity of the SNAP protein, where the polarity becomes smaller and the intramolecular charge transfer is weakened, resulting in a blue shift of the fluorescence wavelength [23]. This result also demonstrated that the ratiometric fluorescence signal was emitted by SNAP protein binding.

In addition to improving the selectivity of recognition, the ratiometric fluorescent signal can also establish an internal standard to provide quantitative information on the target recognized by the probe. In the magnified images of cell nuclei imaging shown in Figs. 2e and j, the distribution of the ratiometric fluorescence signals with large differences in the nucleus can be clearly seen, and the ratiometric signal value of each imaging point can also be given by positioning (Figs. 2m and n). This is due to the different microenvironments of the probes leading to different abilities of excited state proton transfer, and this difference just reflected the huge differences in the H2B–SNAP fusion proteins at different positions in the nucleus, although the sequences of these proteins are completely the same.

The ratiometric fluorescence signal of protein imaging in the whole nucleus was used as a fingerprint, and each imaging point

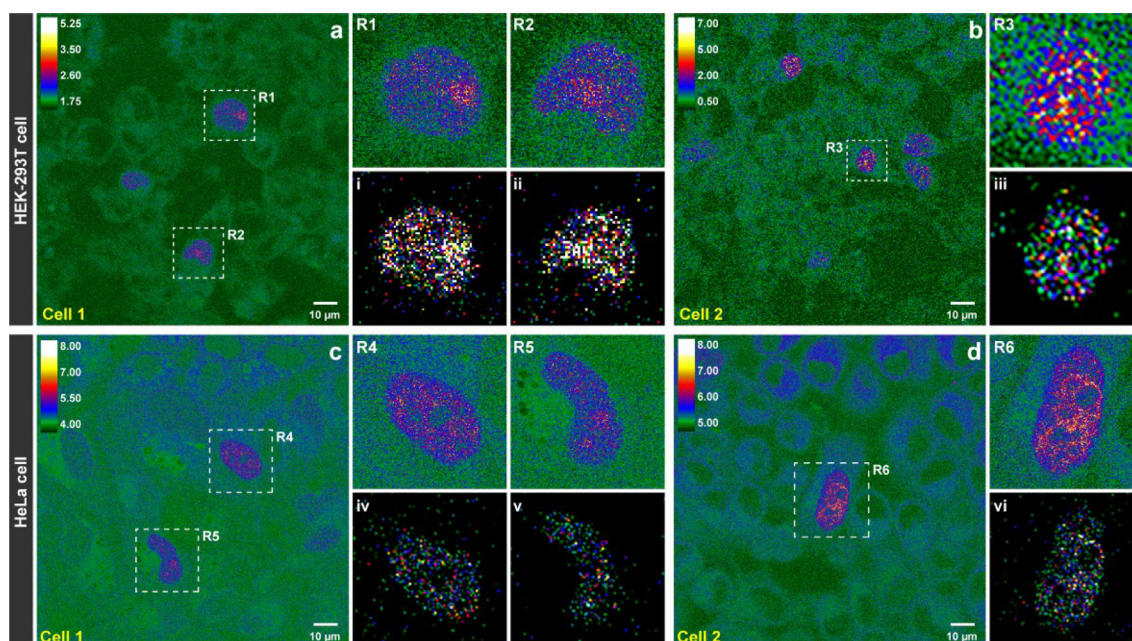


Fig. 3. The ratiometric fluorescence imaging comparison of probe **1** between different cells of the same cell line or different types of cell lines. (a, b) Ratiometric imaging of HEK-293T cells; (c, d) ratiometric imaging of HeLa cells. The R1–R6 were the locally enlarged areas of their left cells, and their ratio fluorescence signals were further adjusted and shown in i–vi. The probe concentration was 1 $\mu\text{mol/L}$, the incubation time was 1 h, and the excitation wavelength was 405 nm. Scale bar: 10 μm .

was used as the details of the map. The comparison of this map was then expected to be used to distinguish cells and discover the details of the intracellular distribution of functional molecules. As shown in Fig. 3, the ratiometric fluorescence imaging comparison between different cells of the same cell line or different types of cell lines, it can be seen that the distribution of H2B–SNAP fusion protein in each nucleus has its characteristics, and the differences between different cell lines are bigger. This ratiometric fluorescent signal fingerprint is expected to establish a logical relationship with the cell dynamic network in the future, to be used to detect or diagnose physiology or pathology.

In summary, we developed a fluorogenic probe for ratiometric recognition of SNAP-tag proteins and achieved wash-free fluorescence imaging of target proteins employing genetically encoded technology. The ratiometric fluorescence signal of this probe comes from the fact that when the naphthalimide fluorophore is close to the protein, the hydroxyl group at the 3rd position forms an intermolecular hydrogen bond with the carbonyl group in the protein, resulting in an excited state proton transfer after being excited by light. The ratiometric fluorescence change from blue to red can not only effectively improve the signal-to-noise ratio of imaging to realize wash-free imaging, but also quantitatively give the hydrogen bond strength between the probe and the bound SNAP protein, thereby indicating the microenvironmental differences of SNAP protein at different positions. The use of ratiometric fluorescent protein imaging as a fingerprint is expected to be applied in physiological and pathological diagnosis as image omics in the future.

Declaration of competing interest

The authors declare that they have no known competing financial interests or personal relationships that could have appeared to influence the work reported in this paper.

Acknowledgments

This work is supported by the National Natural Science Foundation of China (Nos. 22225806, 22078314 and 22278394) and Dalian Institute of Chemical Physics (Nos. DICPI202227 and DICPI202142).

Supplementary materials

Supplementary material associated with this article can be found, in the online version, at doi:10.1016/j.ccl.2023.108266.

References

- [1] J. Chen, W. Liu, X. Fang, et al., *Chin. Chem. Lett.* 33 (2022) 5042–5046.
- [2] J. Chen, C. Wang, W. Liu, et al., *Angew. Chem. Int. Ed.* 60 (2021) 25104–25113.
- [3] W. Liu, J. Chen, Q. Qiao, et al., *Chin. Chem. Lett.* 33 (2022) 4943–4947.
- [4] Q. Qiao, W. Liu, J. Chen, et al., *Angew. Chem. Int. Ed.* 61 (2022) e202202961.
- [5] Q. Qiao, W. Liu, Y. Zhang, et al., *Angew. Chem. Int. Ed.* 61 (2022) e202208678.
- [6] C. Li, Y. Xu, L. Tu, et al., *Chem. Sci.* 13 (2022) 6541–6549.
- [7] Y. Xu, C. Li, J. An, et al., *Sci. China Chem.* 66 (2022) 155–163.
- [8] Y. Xu, C. Li, X. Ma, et al., *Proc. Natl. Acad. Sci. U. S. A.* 119 (2022) e2209904119.
- [9] P. Wang, H. Yang, C. Liu, et al., *Chin. Chem. Lett.* 32 (2021) 168–178.
- [10] X. Zhang, L. Wang, N. Li, et al., *Chin. Chem. Lett.* 32 (2021) 2395–2399.
- [11] K. Lang, *J.W. Chin. Chem. Rev.* 114 (2014) 4764–4806.
- [12] W. Chi, Q. Qiao, C. Wang, et al., *Angew. Chem. Int. Ed.* 59 (2020) 20215–20223.
- [13] L. Miao, W. Zhou, C. Yan, et al., *Acta Pharm. Sin. B* 12 (2022) 3739–3742.
- [14] W. Chi, Q. Qi, R. Lee, et al., *J. Phys. Chem. C* 124 (2020) 3793–3801.
- [15] M.E. Norako, M.J. Greaney, R.L. Brutchey, *J. Am. Chem. Soc.* 134 (2012) 23–26.
- [16] S. Leng, Q.L. Qiao, Y. Gao, et al., *Chin. Chem. Lett.* 28 (2017) 1911–1915.
- [17] A. Gautier, A. Juillerat, C. Heinis, et al., *Chem. Biol.* 15 (2008) 128–136.
- [18] W. Liu, Q. Qiao, J. Zheng, et al., *Biosens. Bioelectron.* 176 (2021) 112886.
- [19] Q. Qiao, W. Liu, W. Chi, et al., *Aggregate* (2022), doi:10.1002/agt.2.258.
- [20] C. Wang, W. Chi, Q. Qiao, et al., *Chem. Soc. Rev.* 50 (2021) 12656–12678.
- [21] D. Bu, Y. Wang, N. Wu, et al., *Chin. Chem. Lett.* 32 (2021) 1799–1802.
- [22] S. Wang, B. Zhu, B. Wang, et al., *Chin. Chem. Lett.* 32 (2021) 1795–1798.
- [23] S. Leng, Q. Qiao, L. Miao, et al., *Chem. Commun.* 53 (2017) 6448–6451.